Check for updates

Inter ocean basin moisture fluxes and the onset of the summer rainy season over southern Mexico

Víctor Magaña[1]* and Sonia Diaz[2]

[1]Instituto de Geografía, Universidad Nacional Autónoma de México, Mexico, Mexico, [2]Posgrado en Ciencias de la Tierra, Universidad Nacional Autónoma de México, Mexico, Mexico

The onset of the rainy season in monsoonal climates is a key element for the development of water related activities. In southern Mexico, it starts in late May or early June, while in western and northwestern part of the country in begins between early and mid-July. Previous studies indicate that it depends on the meridional position of the eastern Pacific Inter Tropical Convergence Zone (ITCZ). By mean of analyses of the Vertically Integrated Moisture Flux, the low level atmospheric dynamics in the tropical Americas is analyzed to establish the temporal evolution of inter ocean moisture fluxes that lead to the onset of the summer rainy season in southern Mexico. The onset of the rainy season depends on the longitudinal position of the center of maximum convective activity in the ITCZ, which induces a quasi-stationary low-level cyclonic circulation that results in moisture fluxes to the Mexican Pacific coast and rains. The Caribbean Low-Level Jet (CLLJ) is a mechanism that modulates inter ocean basin moisture fluxes into the eastern Pacific ITCZ and the location of the maximum convective activity in this system. We propose that the sequence of events that leads to the onset of the rainy season in southern Mexico is: (i) an episode of strong moisture flux from the Caribbean Sea into the eastern Pacific ITCZ, (ii) a region of intense convective activity in the ITCZ that triggers a quasi-stationary low-level cyclonic circulation which in turn, induces moisture flux into southern Mexico, and (iii) the development of convective activity in southern Mexico that determines the onset of the rainy season. The intensification of the CLLJ from June to July also results in a westward displacement of the region of maximum convection within the ITCZ that leads to changes in the atmospheric circulations and moisture fluxes that determine the onset of the rainy season at higher latitudes in the Mexican Pacific coast.

Introduction

The characteristics of the rainy season have been the subject of numerous investigations around the world. Determining or predicting the onset of the rainy season is a subject of major interest in tropical and subtropical climates, given its relevance in the planning of several water related activities (e.g., Sivakumar, 1988).

Various methods have been proposed to approximately determine and predict the beginning of summer precipitation regime (e.g., Kousky, 1988; Liebmann and Marengo, 2001; Liebmann et al., 2007; Ferijal et al., 2022). An early or late onset of the rainy season may determine the accumulated precipitation, as in southern Mexico, where it may result in fluctuations of ±10 to 15% with respect to the mean summer accumulated rainfall (Uribe, 2002). A late onset may have negative environmental consequences in terms of water stress in the vegetation and forest fires (Galván and Magaña, 2020) or negative impacts in the rainfed agriculture (Adams et al., 2003; Neri and Magaña, 2015).

Most of Mexico exhibits a monsoonal type of climate with a relatively dry winter from November to April and a rainy season from May through October (Englehart and Douglas, 2002; Higgins et al., 2003), which includes a relative minimum in precipitation between July and August, known as the Mid-Summer Drought (MSD) (Magaña et al., 1999). The MSD involves the temporal evolution of the CLLJ (Amador, 1998) and its effects in the ITCZ (Magaña and Caetano, 2005; Herrera et al., 2015). On interannual time scales, a wet or a dry rainy season in Mexico and Central America depends on El Niño Southern Oscillation (ENSO), which affects the intensity of the CLLJ (Wang, 2007) and the tropical cyclone activity over the Caribbean Sea (Dominguez and Magaña, 2018). It has been suggested that the CLLJ, ENSO and the North Atlantic Subtropical High exhibit a relationship that affects regional climate over most of the northern tropical Americas (Wang, 2007). In particular, the onset of the rainy season in southern Mexico appears to be related to the temporal and spatial characteristics of the eastern Pacific ITCZ (Uribe, 2002), which in turn may be modulated by ENSO on interannual time scales (Magaña et al., 2003).

The meridional migration and intensity of the eastern Pacific ITCZ between May and June determines the initiation of the rainy season along the Mexican Pacific coast. Although the temporal evolution of the eastern Pacific ITCZ is generally controlled by the meridional convergence of low-level moisture and surface boundary conditions, related to the Sea Surface Temperature (SST) gradients (Lindzen and Nigam, 1987), the CLLJ may also be important in the seasonal evolution (location and magnitude) of its intense tropical convection (Méndez and Magaña, 2010; Durán-Quesada, 2012; Herrera et al., 2015). Periods of intense or weak of CLLJ may influence the spatial characteristics of the ITCZ (Herrera et al., 2015) by means of fluctuations in the moisture flux from the Caribbean Sea into the eastern tropical Pacific (García-Martínez and Bollasina, 2020).

Various studies show that El Niño conditions influence the rainy season when the sources and sinks of atmospheric moisture are altered (Magaña et al., 2003). During El Niño boreal summer, the mean position of the ITCZ in the eastern Pacific tends to remain closer to the equator than normal

(Waliser and Gautier, 1993), which tends to result in a late onset of the rainy season in Mexico (Uribe, 2002). Magaña et al. (1999) observed a westward shift in the location of the most intense convection in the eastern Pacific ITCZ during the MSD, which controls tropical and subtropical atmospheric circulations over the Americas. These circulations correspond to forced quasi-stationary cyclonic circulations (Rossby wave) to the northwest of the convective forcing (Gill, 1980), which affect the moisture flux into southern Mexico and the characteristics of the rainy season.

It may be hypothesized that, depending on the intensity and position of convective activity in the ITCZ, the associated south to north moisture flux from the tropical eastern Pacific to Mexico may vary and consequently, the characteristics of tropical convective activity along its Pacific coast. The sequence of events that may determine the onset of the rainy season include the intensification of the inter ocean moisture flux associated with the CLLJ. Therefore, the objective of the present study is to document such sequence of dynamical processes that contribute to the seasonal evolution of the summer rainy season in the southern Mexico region, including its onset.

Data and methodology

Water vapor flux is important for understanding the global hydrological cycle (Yamada, 2015). Various studies have shown that precipitation events are influenced by the timing, positioning, and duration of vertically integrated water vapor transport (e.g., atmospheric rivers; Gimeno et al., 2014). Its convergence is crucial for the development of events of intense convective activity (e.g, Ejigu et al., 2021). The vertically integrated moisture fluxes (VIMF) (Eq. 1) and its convergence constitute good indicators of changes in precipitable water (PW) and convective activity over the ITCZ and tropical regions with monsoonal climate (Fasullo and Webster, 2003). The VIMF is estimated as:

$$VIMF = \frac{1}{g} \int_{p=1000}^{p=700} \mathbf{V}q \, dp \qquad (1)$$

where q is the specific humidity (kg/kg), $\mathbf{V}$ is the horizontal wind field, g is the gravity constant, and p defines a pressure level. VIMF is calculated using daily ERA-5 data for the 1979–2018 period [Copernicus Climate Change Service (C3S), 2017].

A convergent field of VIMF means an area of moisture sink, while a divergent one constitutes the moisture source. Over short time periods, the VIMF may be interpreted as proportional to moisture advection, as in the tropics. Boundary layer moisture convergence is crucial for the development of deep convection

(Back and Bretherton, 2009). For the present study, the VIMF and the convergence of the VIMF are calculated for the 1,000–700 hPa tropospheric layer to include the boundary layer moisture transport and the potential effect of easterly waves (Serra et al., 2010).

Changes in PW induced by VIMF convergence are important to examine episodes of intense tropical convection in the ITCZ and in the tropical Americas (Durán-Quesada et al., 2017). Daily PW data is obtained using the atmospheric moisture content between 1,000 and 300 hPa by means of the expression:

$$PW = \frac{1}{g} \int\limits_{1000}^{300} q \, dp \qquad (2)$$

Although (Eq. 2) considers the entire atmospheric column, the largest contribution to PW comes from moisture convergence at low atmospheric levels.

Outgoing Longwave Radiation (OLR) data from NOAA/NCEP are used to document deep convective activity in the ITCZ for the 1981–2018 period (NOAA, 2022). The daily OLR data have a spatial resolution of $2.5° \times 2.5°$. Precipitation estimates correspond to the [Tropical Rainfall Measuring Mission (TRMM), 2011] data on a $0.25° \times 0.25$ grid for the period 1998–2018. Data from various weather stations in the Pacific coast of Mexico (CONAGUA-SMN, 2022) are also used as reference to determine the onset of the rainy season.

One of the most popular methods to estimate the onset of the rainy season is the so-called method of "anomalous accumulation" (Liebmann et al., 2007), which is based on the sum of daily precipitation with a positive slope. This method has the advantage that it does not set a threshold for rainfall that should occur in a certain period (Tourigny and Jones, 2009), compared to other methods that require defining magnitude and duration of rainfall for a certain number of days. Therefore, it may be applied independent of the place where the onset of the rainy season is to be calculated.

The difference between two consecutive 10 days composites, corresponding to conditions before and after the onset of the rainy season, or two consecutive monthly means, is used to show the enhancement of the CLLJ, the changes in the eastern Pacific ITCZ and the related moisture fluxes.
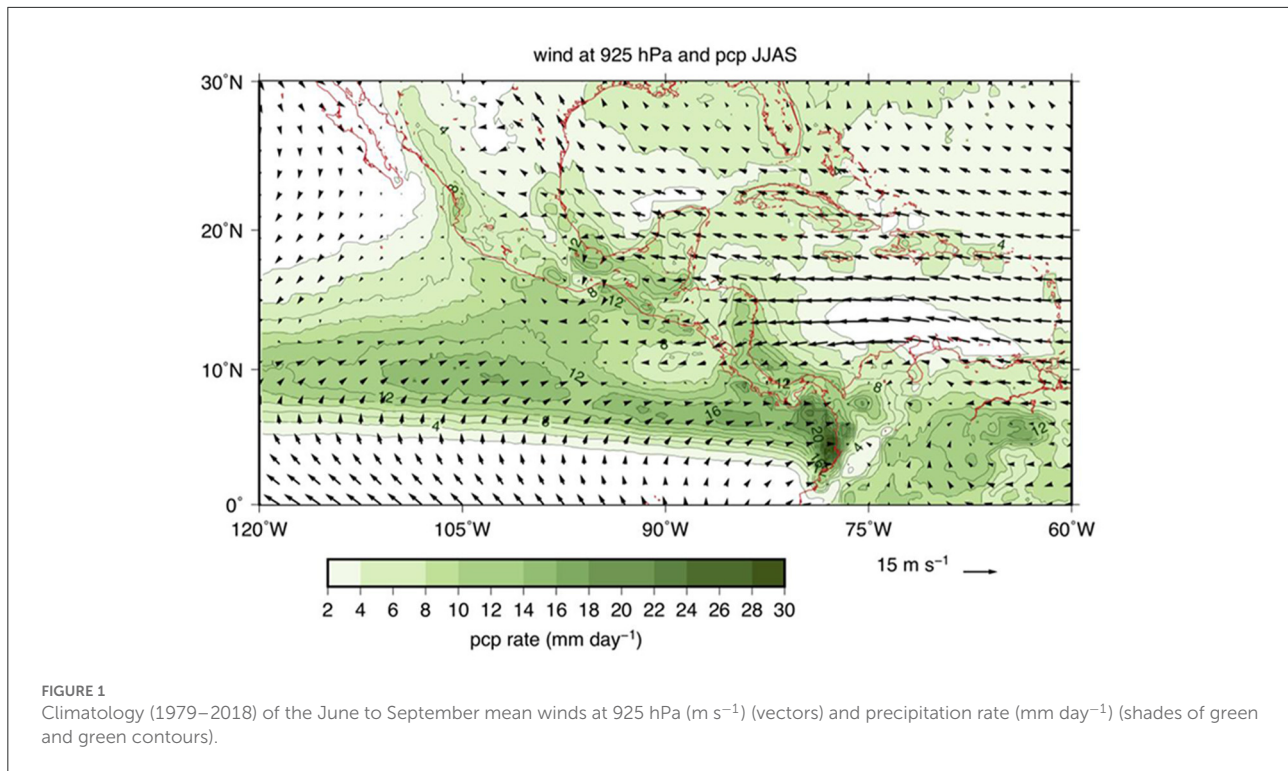
Results

The inter ocean basin moisture fluxes between the Caribbean Sea and the tropical eastern Pacific ITCZ

Over the eastern Pacific, off the coast of Mexico and Central America, the average June to September low-level winds (925 hPa) are generally weak (Figure 1). Between 10 and 12°N, low-level winds converge to maintain the ITCZ, in relation to the low-level branches of the Hadley cells (Hastenrath, 2002). The precipitation rate between 105–120°W and 10–12°N is larger than 10 mm day^{-1}. Over the tropical Atlantic, the mean low-level flow is dominated by easterly winds that intensify over the Caribbean Sea, generating the CLLJ (Amador, 1998). The CLLJ exit region results in low-level convergence that generates a zone of intense precipitation of more than 16 mm day^{-1}. Although the CLLJ is present throughout most of summer, it reaches maximum intensity in July, when it extends to eastern Pacific transporting moisture and contributing to the formation and intensification of the ITCZ, between 95 and 85°W, where precipitation rate is around 16 mm day^{-1}.

In May, the ITCZ extends over the region where the meridional convergence of the VIMF occurs, between 85–140°W and around 8°N (Figure 2A). Over the Caribbean Sea the VIMF is westward and strong associated with the CLLJ and meets with the eastward VIMF over Central America. The VIMF convergence larger than −10 mm day^{-1} maintains PW values over 55 mm in most of the ITCZ. In the CLLJ exit region, over the western Caribbean Sea, the VIMF convergence is around −15 mm day^{-1}, maintaining intense tropical convection (Herrera et al., 2015). In the eastern Caribbean Sea, in the CLLJ entrance region, divergence in the VIMF (5–10 mm day^{-1}) results in weak precipitation rates (<2 mm day^{-1}), even though it corresponds to a climatic warm pool. In June, the ITCZ receives additional moisture from the Caribbean Sea at around 12°N (Figure 2B) since the westward moisture flux through Central America extends to 90°W. The VIMF convergence significantly increases in the CLLJ exit region, leading to PW values of more than 50 mm. July corresponds to the period of maximum strength of the CLLJ (Figure 2C), which results in VIMF that converges at around 90–95°W, 10–12°N with PW values above 50 mm. In the CLLJ exit region, the VIMF convergence maximizes (−25 mm day^{-1}) and results in intense precipitation of more than 500 mm month^{-1} (Herrera et al., 2015). In August, the CLLJ weakens and its influence in the eastern Pacific ITCZ decreases (Figure 2D). The VIMF only extends from the Caribbean Sea to 95°W. The magnitude of the convergence of the VIMF off the Caribbean coast also diminishes.

The intensification of the CLLJ from May to July modulates the moisture flux over the eastern part of the ITCZ and leads to a westward displacement of its most intense convective activity. The weakening of the CLLJ in August and September allows an eastward return of moisture convergence and intense tropical convection in the ITCZ close to the coast of Central America. The mean zonal displacement in the maxima in convective activity in the ITCZ occurs as part of the annual cycle of tropical convection. On time scales of a few days, the episodes of intense convective activity in the ITCZ are related to periods of CLLJ acceleration. For instance, during the year 2000, intense
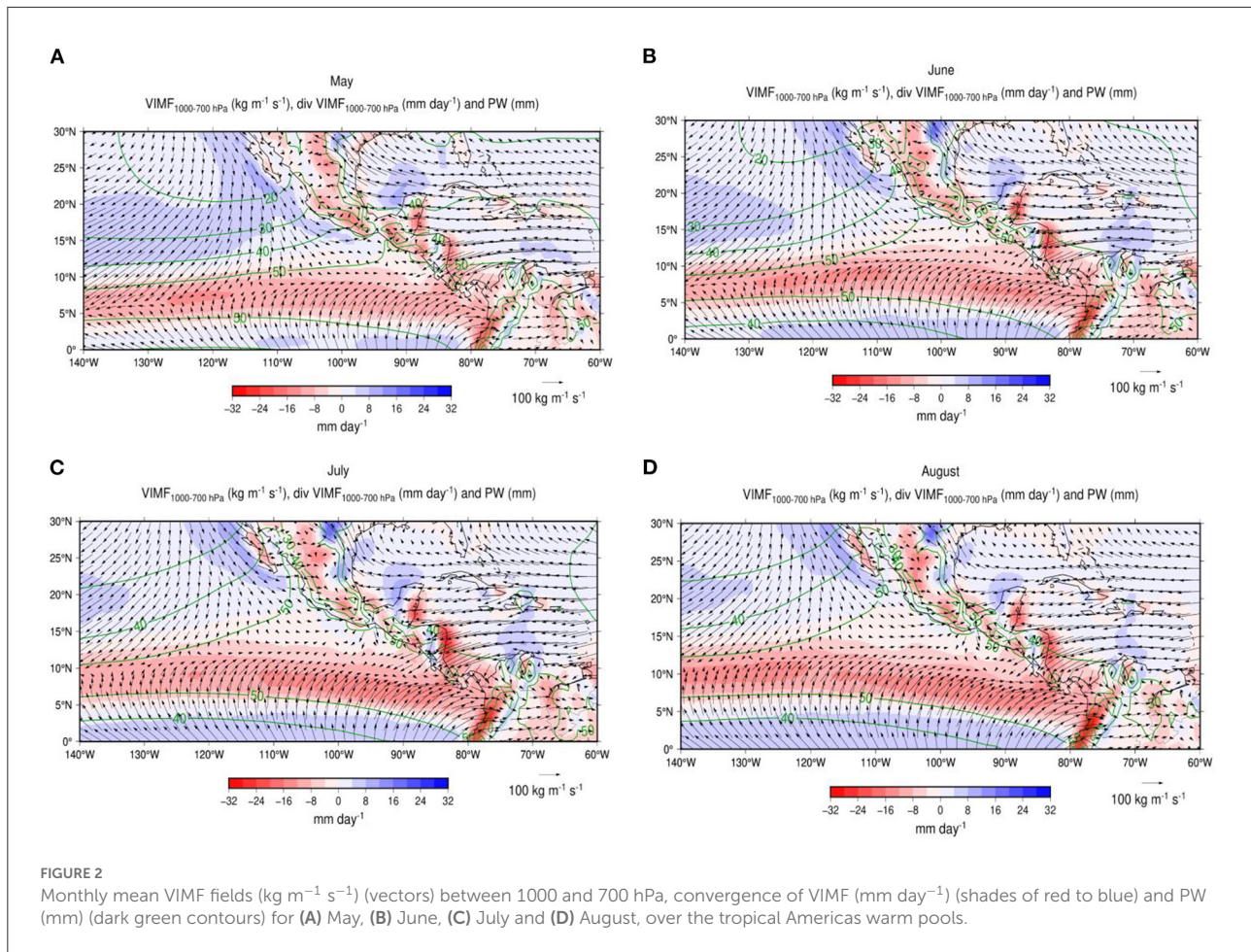
FIGURE 1
Climatology (1979–2018) of the June to September mean winds at 925 hPa (m s^{-1}) (vectors) and precipitation rate (mm day^{-1}) (shades of green and green contours).

convection (OLR $<$ 220 Watt m^{-2}) in the ITCZ (10–12°N) and at the CLLJ exit region varies on monthly and sub-monthly time scales (Figure 3A). From June to August, episodes of a few days with intense convective activity in the ITCZ move westward from 90–100°W to 110–130°W. In September, as the CLLJ and the associated zonal component of the VIMF weaken, and the intense convective activity in the ITCZ returns to 90–100°W. The reduced moisture convergence between 90 and 100°W in July, results in a relative minimum in convective activity, corresponding to the MSD (Magaña and Caetano, 2005).

When the VIMF associated with the CLLJ intensifies, between Julian days 143 and 154 of the year 2000 (Figure 3A), the westward and eastward components of the VIMF in the eastern Pacific converge, between 90 and 95°W, and produce deep tropical convection in the ITCZ. During this period, the onset of the summer rainy season in southern Mexico occurs (Julian day 148). A similar sequence of processes occurs in other years, for instance between Julian days 166 and 176 of 2005 (Figure 3B), when the zonal acceleration of the VIMF related to the CLLJ lead to moisture convergence and an episode of intense convection in the ITCZ between 90–100°W. In this year, the rainy season in southern Mexico began around Julian day 169, which may be consider a late onset since it usually occurs during the 1st week of June. In general, summer rains in southern Mexico begin when intense tropical convective activity in the ITCZ around 90°W occurs. The VIMF convergence, as large as

30 mm day^{-1}, enhances the ITCZ as a moisture source for the northeastern tropical Pacific region.

During the rest of the summer season, episodes of CLLJ acceleration result in intense zonal VIMF from the Caribbean into the eastern Pacific and recurrent bursts of tropical convection in the ITCZ. As the deep tropical convection extends westward, summer rains in southern Mexico and parts of Central America tend to diminish between 85 and 100°W, which corresponds to the MSD.

The enhancement of the ITCZ and the westward migration of the maximum deep tropical convection along 10–12°N may be traced following the lowest values of OLR. From May through September, OLR is generally above 230 Watt m^{-2} over the eastern Caribbean Sea (70–60°W), indicating weak convective activity (Figure 4). In the western Caribbean Sea (85–83°W), deep convective activity occurs, spatially fixed at the CLLJ exit region, with OLR values below 200 Watt m^{-2} throughout summer. Intense convective activity in the eastern Pacific ITCZ (105–95°W) is observed from June through September. The corresponding minimum in OLR is around 205 Watt m^{-2} and its longitudinal position migrates from east to west between June and July, and back to the east between August and September. In this way, in May, the mean OLR along the eastern tropical Pacific is usually above 230 Watt m^{-2}, which corresponds to the absence intense convective activity. However, in June intense convection develops along the ITCZ and the minimum values

FIGURE 2
Monthly mean VIMF fields (kg m^{-1} s^{-1}) (vectors) between 1000 and 700 hPa, convergence of VIMF (mm day^{-1}) (shades of red to blue) and PW (mm) (dark green contours) for **(A)** May, **(B)** June, **(C)** July and **(D)** August, over the tropical Americas warm pools.

of OLR are around 98.75°W. By July, the minimum in OLR (203 Watt m^{-2}) migrates westward to 103.75°W due to the enhancement of the CLLJ along this latitude. By August, the CLLJ weakens and the minimum in OLR (205 Watt m^{-2}) shifts eastwards to around 101.25°W. In September, the OLR minimum (205 Watt m^{-2}) is located between 101.75 and 98.75°W, as the CLLJ further weakens.

The eastern Pacific ITCZ acts as a convective heating region off the equator, that induces regional quasi-stationary circulations in the tropical and subtropical Americas, as in the Gill (1980) model. The temporal evolution in the location and intensity of maximum tropical convective activity in the ITCZ reflects in changes of the forced quasi-stationary low-level circulations over the Mexican Pacific (Figure 5A). The corresponding changes in the month-by-month fields of VIMF, its convergence and in precipitation show the evolution toward the onset of the rainy season in Mexico. In this way, from May to June, there is a northward shift, from 8 to 10°N, in the meridional convergence of the VIMF that also displaces the mean position of the ITCZ. The largest increase in precipitation now occurs south of Mexico and west of Central America. This increase in precipitation in southern Mexico includes

the episode of the onset of the summer rainy season. The enhancement of the ITCZ around 10°N in June, with respect to May, forces a cyclonic quasi-stationary circulation in the tropics and subtropics (centered around 112°W, 28°N), with a transition to moisture flux with a slight southerly component from the eastern ITCZ (between 110 and 100°W), that converges in southern Mexico. This resembles the response of the low-level tropical and subtropical atmosphere when the convective forcing is located off the equator (Gill, 1980) (Figure 5B).

From June to July, the ITCZ migrates further north and west, resulting in an enhancement of moisture convergence and convective activity between 110 and 130°W. South of Mexico and west of Central America (100–90°W, 10–12°N), moisture convergence decreases which results in a weakening of tropical convection and the MSD. The intensification in the CLLJ leads to an inter ocean teleconnection between Caribbean Sea and eastern Pacific, and a westward displacement of VIMF convergence that increases precipitation between 100–130°W and 12–14°N (Figure 6). The westward displacement in maximum convective activity in the ITCZ leads to a new quasi-stationary response in the VIMF field that shows as a cyclonic circulation at low levels further west. The intensified CLLJ also
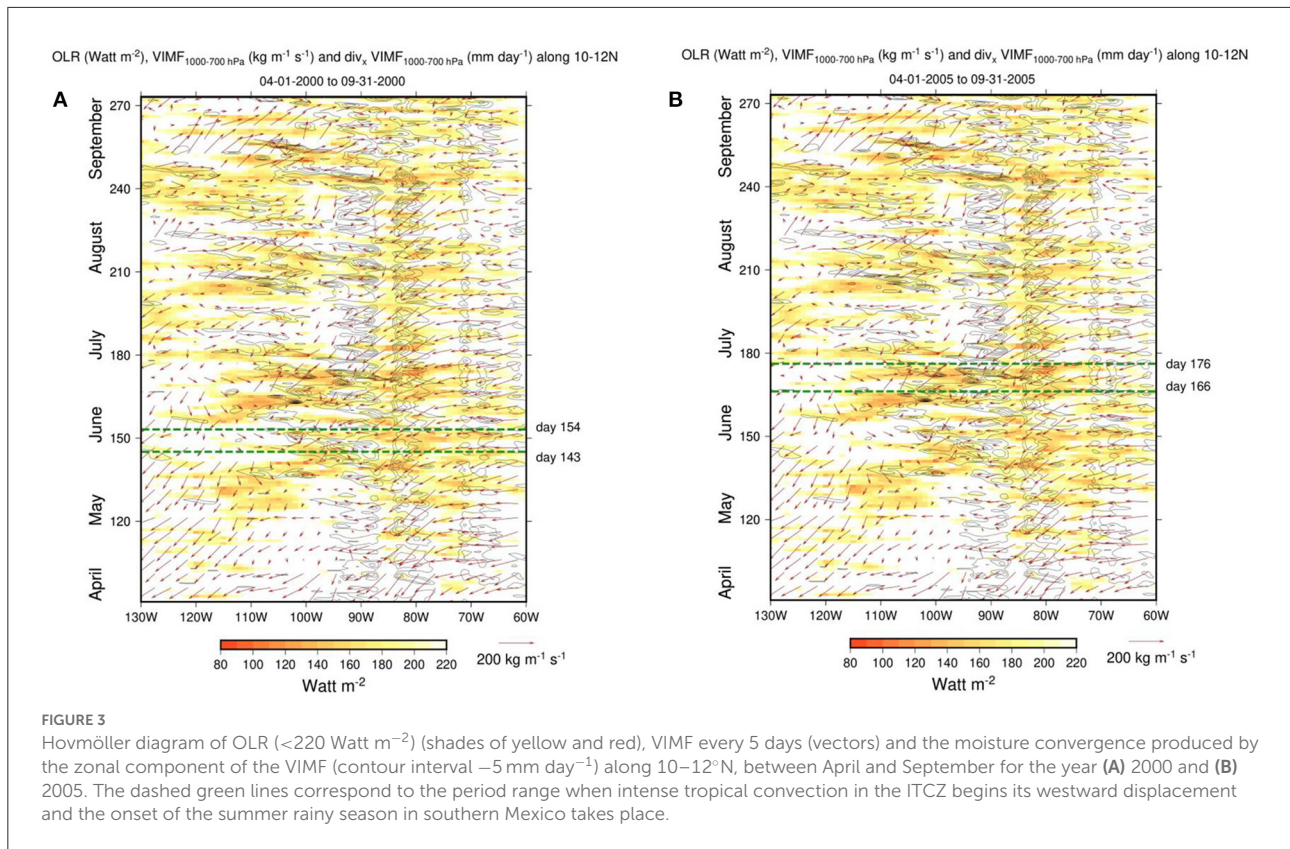
OLR (Watt m⁻²), VIMF$_{1000-700\,hPa}$ (kg m⁻¹ s⁻¹) and div$_x$ VIMF$_{1000-700\,hPa}$ (mm day⁻¹) along 10-12N

FIGURE 3
Hovmöller diagram of OLR (<220 Watt m^{-2}) (shades of yellow and red), VIMF every 5 days (vectors) and the moisture convergence produced by the zonal component of the VIMF (contour interval −5 mm day^{-1}) along 10−12°N, between April and September for the year **(A)** 2000 and **(B)** 2005. The dashed green lines correspond to the period range when intense tropical convection in the ITCZ begins its westward displacement and the onset of the summer rainy season in southern Mexico takes place.
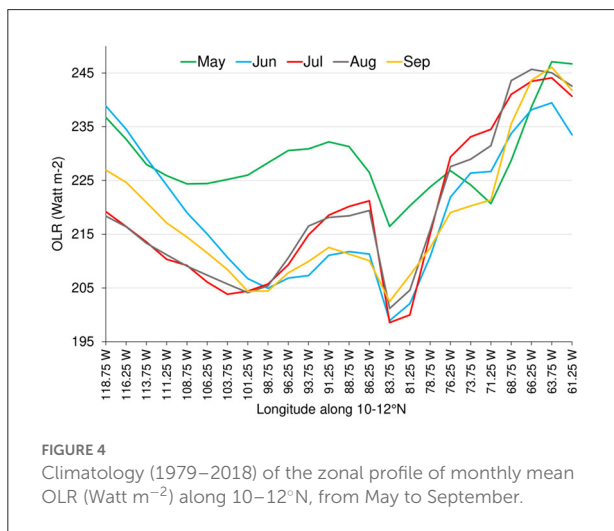
FIGURE 4
Climatology (1979−2018) of the zonal profile of monthly mean OLR (Watt m^{-2}) along 10−12°N, from May to September.
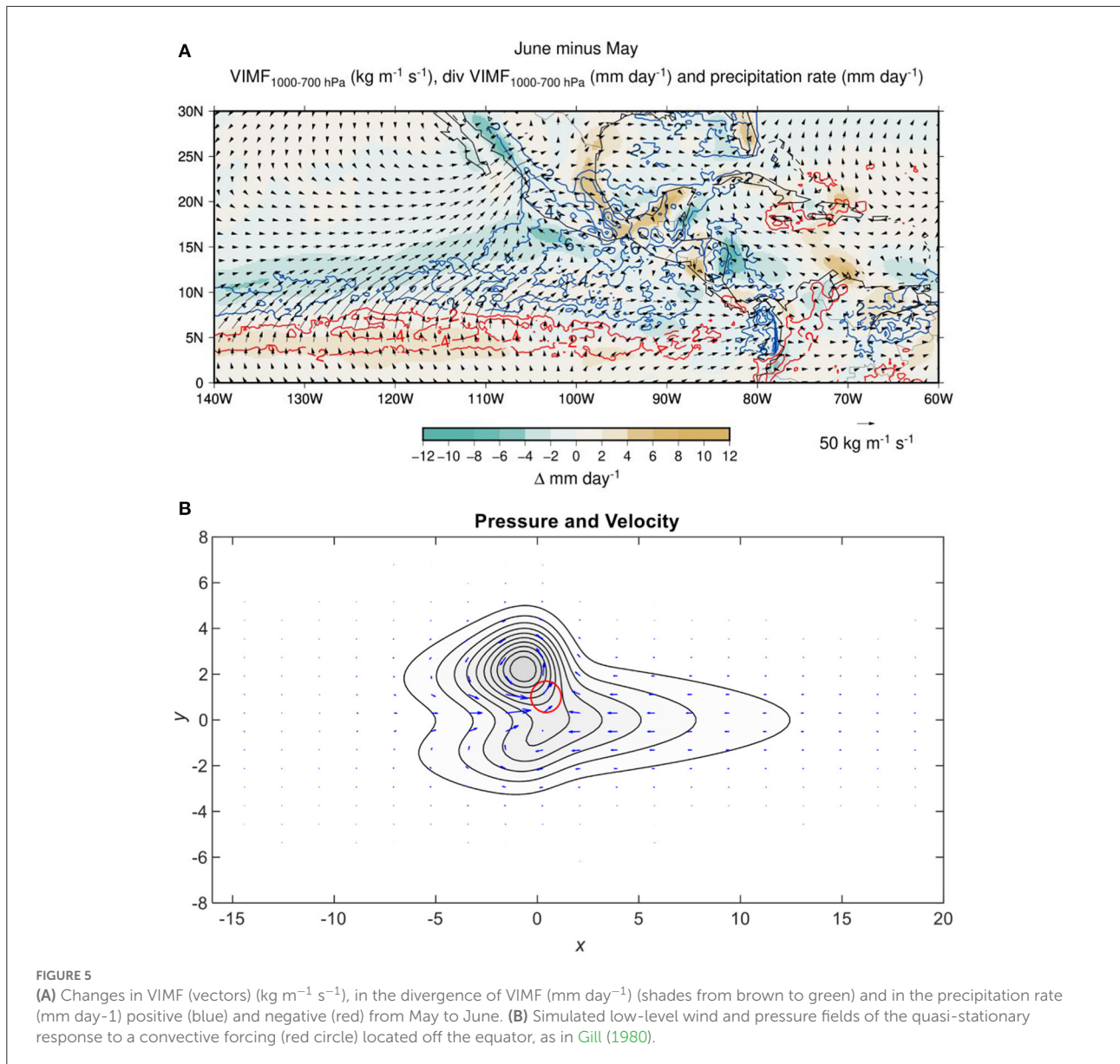
increases VIMF convergence in the jet exit region and results in a maximum in precipitation over the Caribbean coast. In the subsequent months, the CLLJ weakens (not shown), and so the inter ocean moisture flux, allowing the VIMF convergence to retreat to the eastern part of the ITCZ, south of Mexico and west of Central America, ending the MSD period.

The effect of the CLLJ over the ITCZ constitutes an example on how the inter ocean moisture transport results in the

modulation of the annual cycle of tropical convection in the eastern Pacific, even when this atmospheric teleconnection does not necessarily involve large scale quasi-stationary waves, as those discussed by Karoly and Hoskins (1983).

The onset of the summer rainy season along the Pacific coast of Mexico

The onset of the rainy season along the southern part of the Mexican Pacific coast tends to occur during late May or the 1st week of June. Further north and up to the Mexican monsoon region, the onset of the rainy season takes place during mid to late June and during the early part of July (Higgins et al., 1999). The onset may be associated with the 1st day of a 10 day period when the accumulated precipitation shows a trend larger than 2 mm day^{-1} and it rains in at least five out of those 10 days, similar to what Boyard-Micheau et al. (2013) proposed. Intense convective activity usually occurs in the ITCZ around 12°N, 90°W, prior to the onset of the rainy season in southern Mexico. When a pulse in VIMF from the Caribbean Sea enhances deep convection in the ITCZ (moisture source region), the resulting diabetic heating triggers a low-level cyclonic circulation that transports moisture into southern Mexico (moisture sink region). The bursts of intense convection

FIGURE 5
(A) Changes in VIMF (vectors) (kg m^{-1} s^{-1}), in the divergence of VIMF (mm day^{-1}) (shades from brown to green) and in the precipitation rate (mm day-1) positive (blue) and negative (red) from May to June. **(B)** Simulated low-level wind and pressure fields of the quasi-stationary response to a convective forcing (red circle) located off the equator, as in Gill (1980).
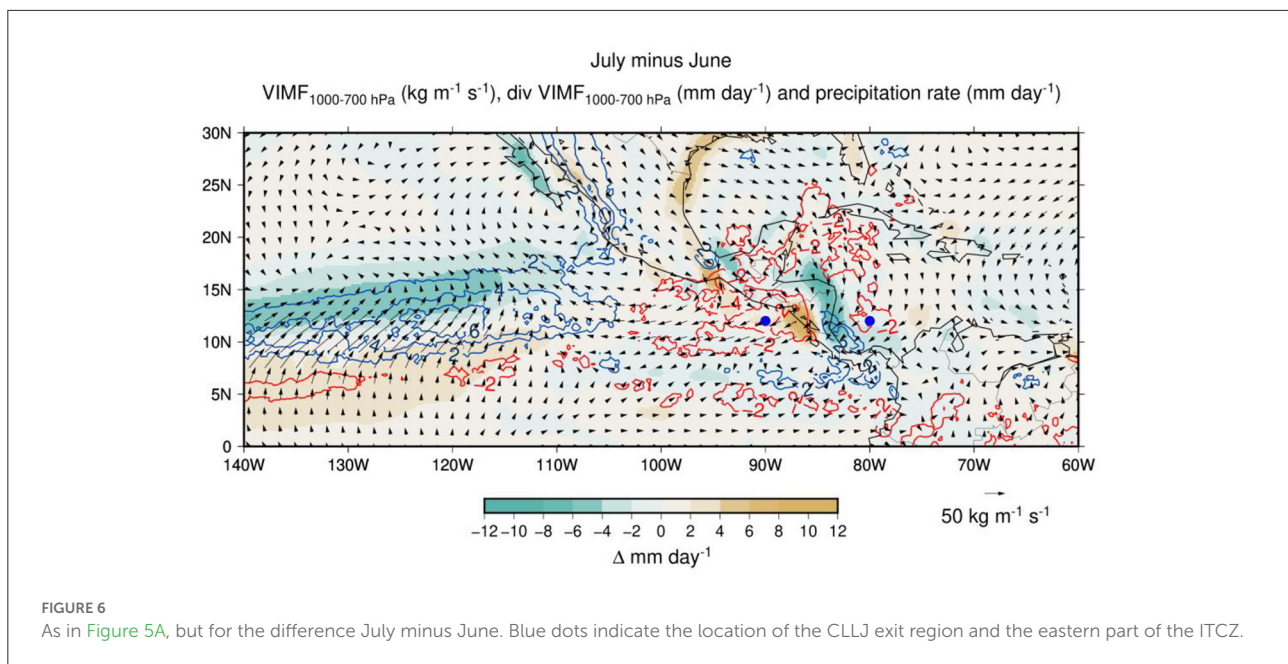
in the ITCZ are recurrent, but in late May there is enough atmospheric moisture convergence in southern Mexico as to produce continuous rains that correspond to the beginning of the summer rains.

The periodicity of the episodes of intense winds across Central America may be determined by means of power spectral analyses of the zonal component of the wind at 925 hPa, u_{925}, at 80°W, 12°N (Figure 7A) and at 90°W, 12°N (Figure 7B). The first point corresponds to the CLLJ exit region while the second one reflects the increase of momentum when the CLLJ extends to the eastern Pacific. Results indicate that there is significant high frequency variability in u_{925} in the period range of less than 10 days in both locations, with spectral peaks with frequencies around 1/5 and 1/8 days^{-1}. The variability in the

5 days period range is related to easterly waves (Serra et al., 2008). Most important, the high frequency fluctuations in the zonal wind in the CLLJ exit region and the eastern Pacific are coherent (Figure 7C), with pulses in Caribbean leading those in the eastern tropical Pacific. The largest coherence is in the low frequency part of the spectrum, reflecting the slow effect of the intensification of the CLLJ that extends over the eastern Pacific during summer. The squared coherence between u_{925} at these locations in various frequencies is also significant, indicating that accelerations (decelerations) in the zonal flow across Central America acts as an inter ocean basin atmospheric teleconnection.

The CLLJ – ITCZ teleconnection may also be observed by means of a modified Hovmöller diagram. In this analysis the

FIGURE 6

As in Figure 5A, but for the difference July minus June. Blue dots indicate the location of the CLLJ exit region and the eastern part of the ITCZ.

traditional Hovmöller diagram is modified to a time-longitude lag-correlation diagram to yield statistically relevant estimates of zonal wavelengths, phase and group velocities (Fraedrich and Lutz, 1987). Using band-passed (10 to 3 days period) u_{925} at 80°W, 12°N as a reference point in the CLLJ exit region (Figure 8A), it is observed the signal in u_{925} propagates from 60°W to 100°W in 4 to 5 days and extends from the CLLJ into the tropical eastern Pacific. When the reference point is in the eastern Pacific (90°W, 12°N) (Figure 8B), it is confirmed that the changes in the low-level zonal winds originate in the Caribbean region and extend downstream to approximately 120°W in about 5 days.

Various analysis (e.g., Hastenrath, 2002) have shown that the moisture flux convergence (>32 mm day^{-1}) from the subtropics maintains the eastern Pacific ITCZ. However, the contribution of moisture from the Caribbean Sea to the ITCZ is also important, since the recurrent VIMF fluxes from the CLLJ may induce moisture convergence as large as 20 mm day^{-1}. Usually, these pulses in the zonal component of VIMF from the Caribbean result in bursts of intense convection that last for several days. A previously shown, a few days (around 5 days), prior to the onset of the rainy season, convective activity in the ITCZ enhances. A backwards trajectory analysis for these days, with reference point in the eastern Pacific ITCZ (95°W, 10°N, 500 masl) (Figure 9) indicates that parcels that contribute to moisture convergence come from the Southern and Northern eastern Pacific subtropics. However, there are also numerous parcels that come from the Caribbean Sea into the ITCZ to produce episodes of intense convection. These parcels tend to cross from the Caribbean Sea into the eastern Pacific along the so-called

Isthmus of Papagayo in Central America, constituting a form of gap flow.

The transition in the atmospheric conditions, calculated as the difference between 10 days after and before the onset of the rainy season in southern Mexico (Figure 10), shows that the inter ocean low-level (925 hPa) moisture flux strengthens along with moisture convergence and precipitation in the eastern Pacific, south of Mexico (105–100°W, 5–10°N), enhance. The average value of total OLR for the complete 20 days period of this analysis indicates the approximate location of the intense convective heating that forces a cyclonic quasi-stationary circulation, as in the Gill (1980) model. The forced quasi-stationary Rossby wave (centered at 123°W, 20°N) induces southwesterly moisture flux that convergences in southern Mexico to produce precipitation for the beginning of the summer rainy season.

The onset of rainy season in western and northwestern Mexico occurs between mid-June and early July. The temporal evolution of the summer rains along the Pacific coast of Mexico involves ocean-atmosphere interactions. This may be observed by calculating the difference in OLR, Sea Surface Temperature (SST) and surface winds between July and June (Figure 11). It is observed that convective activity develops along northwestern Mexico in relation to the North American Monsoon, while it decreases south of southern Mexico, in relation to the MSD. The eastern Pacific subtropical high weakens given the induced cyclonic quasi-stationary circulation centered around 130°W, 20°N. The weakened northward winds along the Baja Peninsula reduce the Ekman transport and lead to a SSTs increase of around to 3°C in the Pacific coast of Baja and the Gulf of
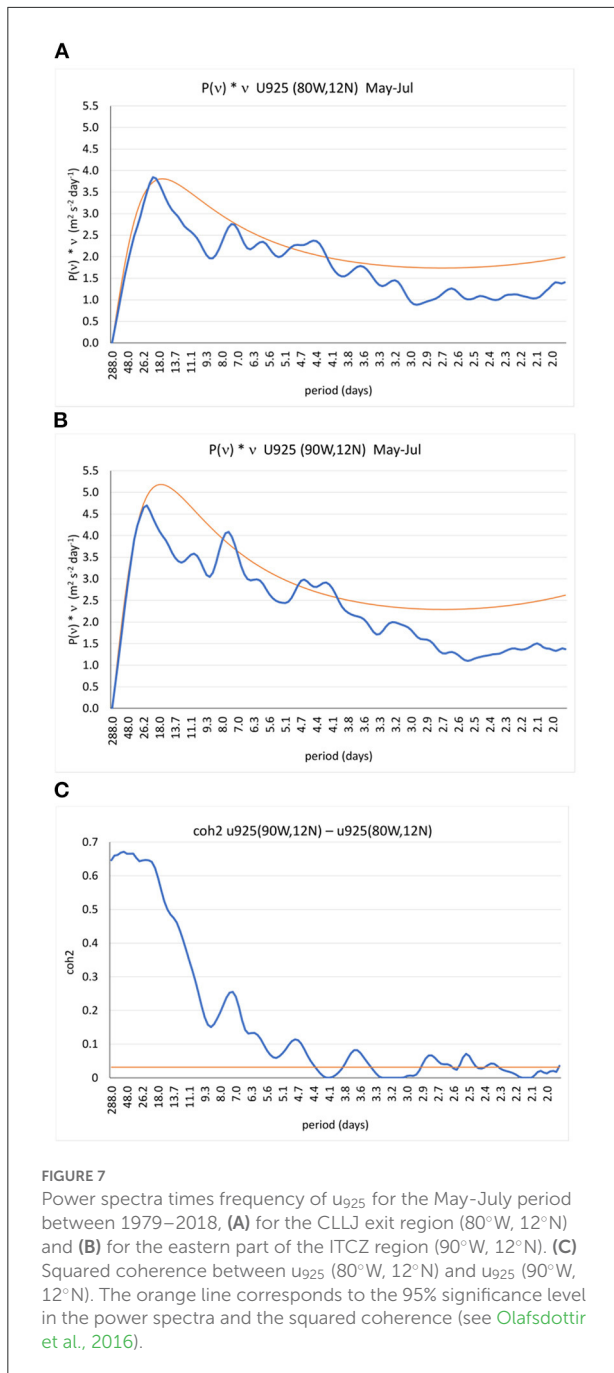
California. A larger meridional SST gradient in the eastern
Pacific determines the mean position of the ITCZ (Lindzen and
Nigam, 1987). In July, the ITCZ displaces further north and with
warmer SSTs in the Pacific, off the coast of northwestern Mexico
and warmer air temperatures and more moisture near the
surface, deep tropical convection occurs in the North American
Monsoon region.

In this way, along with the intense July CLLJ, moisture
convergences and availability result in an increase of PW that
allows the onset of the summer rainy season in northwestern
Mexico. Therefore, the dynamics of the North American
Monsoon could be influence by the seasonal evolution of the
eastern Pacific ITCZ and the intensity of the moisture flux from
the Caribbean, as well as the regional air-sea interactions during
the boreal summer season.

Summary and conclusions

The summer rainy season along the Mexican Pacific
region is largely influenced by low-level atmospheric moisture
fluxes modulated by large scale conditions (e.g., forced quasi-
stationary circulations or SSTs). The onset of the rainy
season in southern Mexico takes place in late May - early
June and progresses over time to northwestern Mexico until
early July, when the North American Monsoon begins.
The intensity of the CLLJ and convective activity in the
eastern Pacific ITCZ are key elements in the establishment of
moisture flux to Mexico and consequently in the onset of the
rainy season.

In the present work, it has been shown that as the CLLJ
intensifies, more moisture is transported from the Caribbean
Sea to the eastern Pacific, making convective activity in the
ITCZ stronger. A more intense zonal moisture flux from
the Caribbean shifts the moisture convergence to the west
and the associated strong convective activity in the ITCZ,
modifying the tropical and subtropical low-level atmospheric
circulations. This is observed in the transition from June
to July, when the CLLJ reaches its maximus intensity and
tropical convection off the Pacific coast of Central America
weakens, resulting in the MSD. The ITCZ constitutes a mean
to trigger a cyclonic quasi-stationary circulation, corresponding
to a Rossby wave in the tropical-subtropical region, that
modifies the mean low-level atmospheric flow that brings
moisture close to southern Mexico that initiates the summer
rainy season.

In summary, in late May and early June, the sequence
of events that results in the onset of the rainy season
in southern Mexico is: (i) enhancement of the CLLJ
and increased inter ocean moisture transport from the
Caribbean Sea to the eastern Pacific, (ii) stronger moisture
convergence in the eastern Pacific ITCZ and deep tropical
convection that acts as a heat convective forcing, that (iii)
triggers a low-level cyclonic quasi-stationary circulation
with enhanced southerly moisture flux into the southern
part of Mexico, and (iv) enhanced moisture convergence
along Mexican Pacific coast that establishes the summer
rains regime.

As the most intense tropical convection in the ITCZ
shifts westward, the induced subtropical cyclone weakens the
dominant Pacific Subtropical High allowing more atmospheric
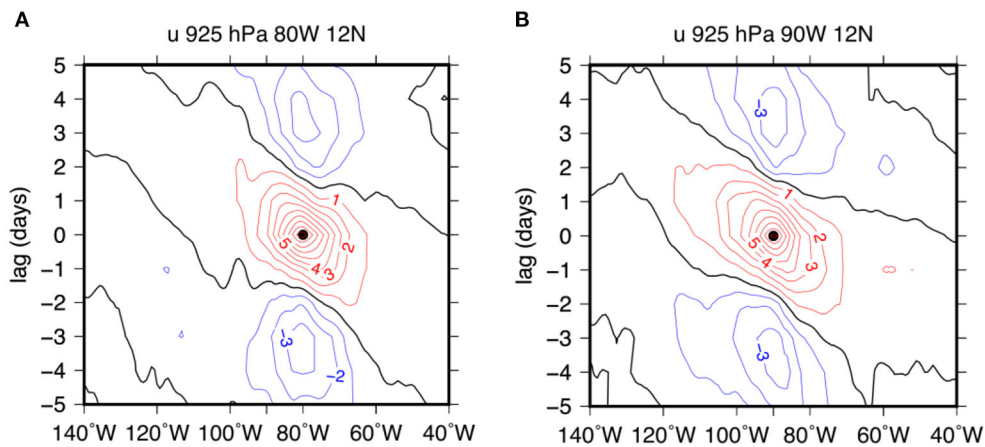moisture around the Baja Peninsula favoring the development

FIGURE 8
Modified time-longitude diagrams for the high frequency (<1/10 days) variations in the zonal wind at 925 hPa (u_{925}) along 12°N, for the period May to July, when the reference point is located at: **(A)** 80°W, 12°N and **(B)** 90°W, 12°N.
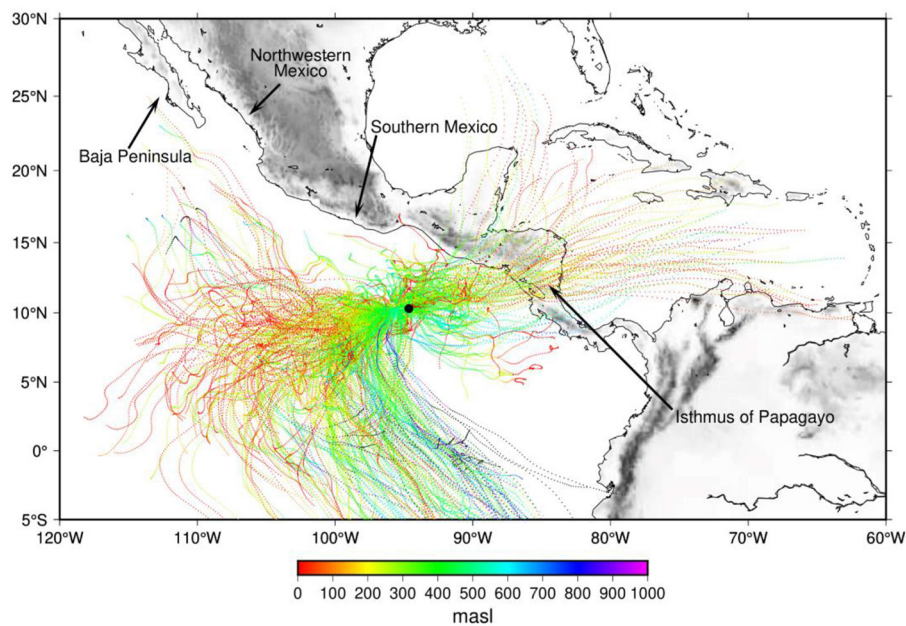

FIGURE 9
Backward trajectory analyses (dotted lines), starting 5 days prior to the onset of the rainy season in southern Mexico, using the 95°W, 10°N region as a reference point (black circle). The colors indicate meters above sea level (masl). The topography in the tropical Americas is in shades of gray.

of tropical convection in northwestern Mexico. This may be an important element to include in the dynamics of the North American Monsoon. It is clear that the dynamics of the eastern Pacific ITCZ is not solely controlled by the moisture flux from the Caribbean, but its influence cannot be neglected in numerous aspects of the annual cycle of climate of Mesoamerica.

The interannual variability in the eastern Pacific ITCZ, mainly determined by ENSO, affects the onset of the rainy season in Mexico and Central America. The tendency for the ITCZ to remain closer to the equator could be the factor that maintains this moisture source more distant from Mexico than normal, not only because anomalously warm SSTs remain closer to the equator, but also because
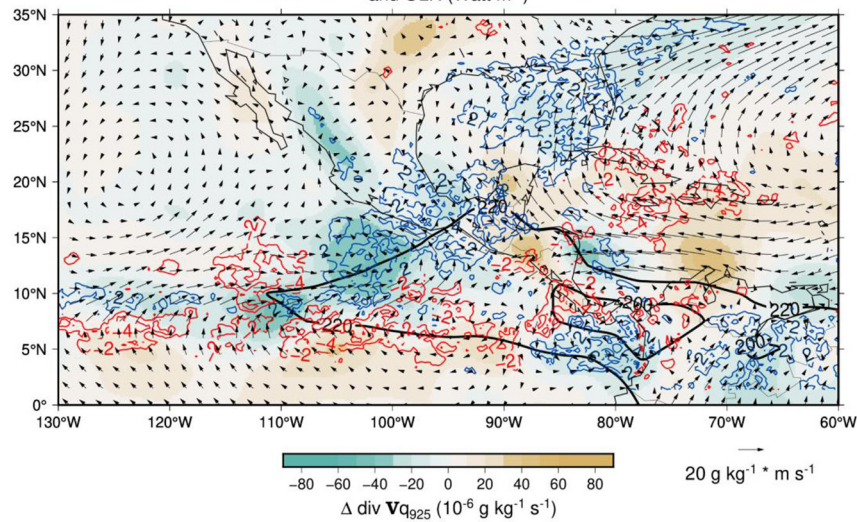
FIGURE 10
Temporal change in the moisture flux at 925 hPa (vectors), its convergence (shades of green to brown) and precipitation (positive lines in blue and negative lines in red) between the average conditions 10 days before and 10 days after the onset of the rainy season in southern Mexico. The black solid line corresponds to the total OLR below 220 Watt m^{-2}) for the 20 days period, as reference for the location of the ITCZ.
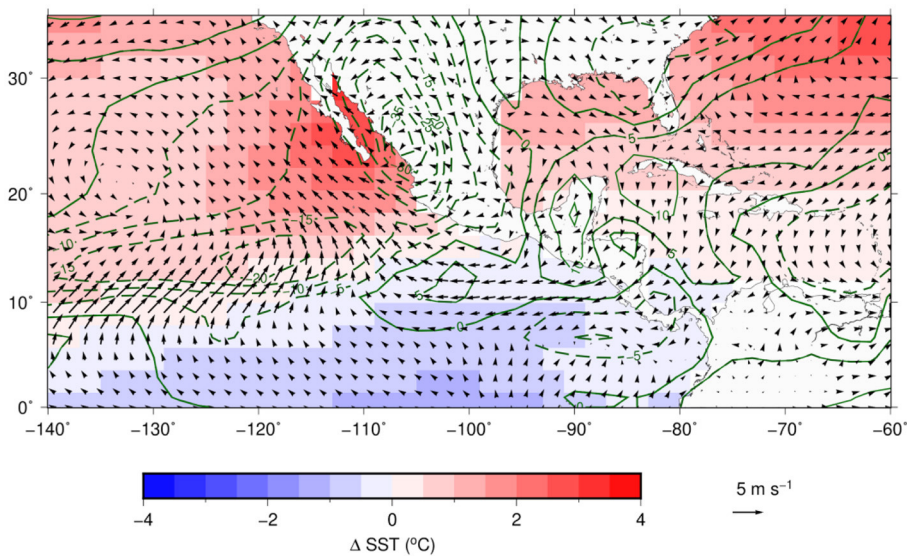

FIGURE 11
Differences (July minus June) in: surface (10 m) winds (vectors), SSTs (shades from blue to red) and OLR (Watt m^{-2}) (green solid lines for positive OLR changes, and green dashed lines for negative OLR changes).

an anomalously strong CLLJ that tends to maintain the ITCZ further west. Exploring the effects of ENSO on the onset of the rainy season in Mexico and its summer climate is an interesting problem of interannual climate variability that may prove to be useful on seasonal regional climate forecasts.

Author's note

Determining the onset of the rainy season is a great value for several water related activities. The present study shows that the inter ocean basin moisture fluxes are important factors that determine not only the onset of the rainy

season but also variations in the summer rains in southern Mexico. The author proposed the methodology followed in the study and implemented the necessary algorithms for the various calculations. The second author tested the proposed ideas about the onset of the rainy season as part of her M.Sc. Thesis. She also prepared most of the final version of the figures.

Data availability statement

Publicly available datasets were analyzed in this study. This data can be found here: https://www.ecmwf.int/; https://iridl.ldeo.columbia.edu/SOURCES/.NOAA/.NCEP/.CPC/.GLOBAL/; https://smn.conagua.gob.mx/es/; https://disc.gsfc.nasa.gov/datasets/TRMM_3B42_Daily_7/summary.

Author contributions

VM: proposal of a mechanism that relates climate variability over the Caribbean Sea with climate variability in the eastern tropical Pacific, hypothesis on how enhancement in the ITCZ leads to convective activity in Mexico. SD: development for a criteria on the onset on the rainy season in southern Mexico, analysis in the shift of maxima in convective activity in the ITCZ and the areas of rain along the Mexican Pacific coast, and development of qualitative model on how variations in the CLLJ affect climate in western Mexico. All authors contributed to the article and approved the submitted version.

Conflict of interest

The authors declare that the research was conducted in the absence of any commercial or financial relationships that could be construed as a potential conflict of interest.

Publisher's note

All claims expressed in this article are solely those of the authors and do not necessarily represent those of their affiliated organizations, or those of the publisher, the editors and the reviewers. Any product that may be evaluated in this article, or claim that may be made by its manufacturer, is not guaranteed or endorsed by the publisher.

References

Adams, R. M., Houston, L. L., McCarl, B. A., Tiscareno, M. L., Matus, J. G., and Weiher, R. F. (2003). The benefits to Mexican agriculture of an El Nino-southern oscillation (ENSO) early warning system. *Agric. Forest Meteorol.* 115, 183–194. doi: 10.1016/S0168-1923(02)00201-0

Amador, J. A. (1998). A climatic feature of the tropical Americas: The trade wind easterly jet. *Top. Meteor. Oceanogr.* 5, 91–102.

Back, L. E., and Bretherton, C. S. (2009). A Simple Model of Climatological Rainfall and Vertical Motion Patterns over the Tropical Oceans. *J. Clim.* 22, 6477–6497. doi: 10.1175/2009JCLI2393.1

Boyard-Micheau, J., Camberlin, P., and Philippon, N. y Moron, V. (2013). Regional-scale rainy season onset detection: A new approach based on multivariate analysis. *J. Clim.* 26, 8916–8928. doi: 10.1175/JCLI-D-12-00730.1

CONAGUA-SMN (2022). Comisión Nacional del Agua - Servicio Meteorológico Nacional. Climatological information. Available online at: https://smn.conagua.gob.mx/es/climatologia/informacion-climatologica/informacion-estadistica-climatologica (accessed January 25, 2022).

Copernicus Climate Change Service (C3S) (2017). ERA5: Fifth generation of ECMWF atmospheric reanalyses of the global climate. Copernicus Climate Change Service Climate Data Store (CDS). Available online at: https://cds.climate.copernicus.eu/cdsapp#!/home (accessed April 1, 2022).

Dominguez, C., and Magaña, V. (2018). The role of tropical cyclones in precipitation over the tropical and subtropical North America. *Front. Earth Sci.* 6, 19. doi: 10.3389/feart.2018.00019

Durán-Quesada, A. M. (2012). *Sources of moisture for Central America and transport based on a Lagrangian approach: variability, contributions to precipitation and transport mechanisms.* Doctoral dissertation. Vigo, Spain: Universidade de Vigo.

Durán-Quesada, A. M., Gimeno, L., and Amador, J. A. (2017). Role of moisture transport for Central American precipitation. *Earth Syst. Dyn.* 8, 147–161. doi: 10.5194/esd-8-147-2017

Ejigu, Y., Teferle, N., Klos, A., Bogusz, J., and Hunegnaw, A. (2021). Monitoring and prediction of hurricane tracks using GPS tropospheric products. *GPS Solutions* 25, 76. doi: 10.1007/s10291-021-01104-3

Englehart, P. J., and Douglas, A. V. (2002). Mexico's summer rainfall patterns: an analysis of regional modes and changes in their teleconnectivity. *Atmósfera* 15, 147–164.

Fasullo, J., and Webster, P. (2003). A hydrological definition of indian monsoon onset and withdrawal. *J. Clim.* 16, 3200–3211. doi: 10.1175/1520-0442(2003)016<3200a:AHDOIM>2.0.CO;2

Ferijal, T., Batelaan, O., Shanafield, M., and Alfahmi, F. (2022). Determination of rainy season onset and cessation based on a flexible driest period. *Theor. Appl. Climatol.* 148, 91–104. doi: 10.1007/s00704-021-03917-1

Fraedrich, K., and Lutz, M. (1987). A modified time-longitude diagram applied to 500 mb heights along 50° north and south. *Tellus A: Dyn. Meteorol. Oceanogr.* 39, 25–32. doi: 10.3402/tellusa.v39i1.11736

Galván, L., and Magaña, V. (2020). Forest fires in Mexico: an approach to estimate fire probabilities. *Int. J. Wildl. Fire* 29, 753–763. doi: 10.1071/WF19057

García-Martínez, I. M., and Bollasina, M. A. (2020). Sub-monthly evolution of the Caribbean Low-Level Jet and its relationship with regional precipitation and atmospheric circulation. *Clim. Dyn.* 54, 4423–4440. doi: 10.1007/s00382-020-05237-y

Gill, A. E. (1980). Some simple solutions for heat-induced tropical circulation. *Quart. J. Roy. Meteor. Soc.* 106, 447–462. doi: 10.1002/qj.49710644905

Gimeno, L., Nieto, R., Vázquez, M., and Lavers, D. A. (2014). Atmospheric rivers: A mini-review. *Front. Earth Sci.* 2, 2. doi: 10.3389/feart.2014.00002

Hastenrath, S. (2002). The intertropical convergence zone of the eastern pacific revisited. *Int. J. Climatol.* 22, 347–356. doi: 10.1002/joc.739

Herrera, E., Magaña, V., and Caetano, E. (2015). Air–sea interactions and dynamical processes associated with the midsummer drought. *Int. J. Climatol.* 35, 1569–1578. doi: 10.1002/joc.4077

Higgins, R. W., Chen, Y., and Douglas, A. V. (1999). Interannual variability of the North American warm season precipitation regime. *J. Clim.* 12, 653–680. doi: 10.1175/1520-0442(1999)012<0653:IVOTNA>2.0.CO;2

Higgins, W. R., Douglas, A., Hahmann, A., Berbery, E. H., Gutzler, D., Shuttleworth, J., et al. (2003). Progress in pan american CLIVAR research: the north american monsoon system. *Atmósfera* 16, 29–65.

Karoly, D., and Hoskins, B. (1983). The steady, liner response of the stratosphere to tropospheric forcing. *Quart. J. Roy. Meteor. Soc.* 109, 455–478. doi: 10.1002/qj.49710946103

Kousky, V. E. (1988). Pentad outgoing longwave radiation climatology for the South American sector. *Reiv. Brasileira Meteorol.* 3, 217–231.

Liebmann, B., Camargo, S. J., Seth, A., Marengo, J. A., Carvalho, L. M. V., Allured, D., et al. (2007). Onset and end of the rainy season in South America in observations and the ECHAM 4.5 atmospheric general circulation model. *J. Clim.* 20, 2037–2050. doi: 10.1175/JCLI4122.1

Liebmann, B., and Marengo, J. A. (2001). Interannual variability of the rainy season and rainfall in the Brazilian Amazon Basin. *J. Clim.* 14, 4308–4318. doi: 10.1175/1520-0442(2001)014<4308:IVOTRS>2.0.CO;2

Lindzen, R. S., and Nigam, S. (1987). On the role of sea surface temperature gradients in forcing low-level winds and convergence in the tropics. *J. Atmos. Sci.* 44, 2418–2436. doi: 10.1175/1520-0469(1987)044<2418:OTROSS>2.0.CO;2

Magaña, V., Amador, J. A., and Medina, S. (1999). The midsummer drought over Mexico and central America. *J. Clim.* 12, 1577–1588. doi: 10.1175/1520-0442(1999)012<1577:TMDOMA>2.0.CO;2

Magaña, V., and Caetano, E. (2005). Temporal evolution of summer convective activity over the America warm pools. *Geophys. Res. Lett.* 32, L02803. doi: 10.1029/2004GL021033

Magaña, V., Vázquez, J. L., Pérez, J. L., and Pérez, J. B. (2003). Impact of El Niño on precipitation in Mexico. *Geofís. Int.* 42, 313–330. doi: 10.22201/igeof.00167169p.2003.42.2.269

Méndez, M., and Magaña, V. (2010). Regional aspects of prolonged meteorological droughts over Mexico and Central America. *J. Clim.* 23, 1175–1188. doi: 10.1175/2009JCLI3080.1

Neri, C., and Magaña, V. (2015). Estimation of vulnerability and risk to meteorological drought in Mexico. *Weather, Clim. Soc.* 8. 151208152610001. doi: 10.1175/WCAS-D-15-0005.1

NOAA (2022). Daily (non-interpolated) Outgoing Longwave Radiation (OLR) data provided by the NOAA PSL, Boulder, Colorado, USA. Available online at: https://psl.noaa.gov (accessed March 10, 2022).

Olafsdottir, K. B., Schulz, M., and Mudelsee, M. (2016): REDFIT-X: Cross-spectral analysis of unevenly spaced paleoclimate time series. *Comput. Geosci.* 91, 11–18. doi: 10.1016/j.cageo.2016.03.001

Serra, Y. L., Kiladis, G. N., and Cronin, M. (2008). Horizontal and Vertical Structure of Easterly Waves in the Pacific ITCZ. *J. Atmosph. Sci.* 65, 1266–1284. doi: 10.1175/2007JAS2341.1

Serra, Y. L., Kiladis, G. N., and Hodges, K. I. (2010). Tracking and mean structure of easterly waves over the Intra-Americas Sea. *J. Clim.* 23 4823–4840. doi: 10.1175/2010JCLI3223.1

Sivakumar, M. V. K. (1988). Predicting rainy season potential from the onset of rains in Southern Sahelian and Sudanian climatic zones of West Africa. *Agric. Forest Meteorol.* 42, 295–305. doi: 10.1016/0168-1923(88)90039-1

Tourigny, E., and Jones, C. (2009). An analysis of regional climate model performance over the tropical Americas. Part II: Simulating subseasonal variability of precipitation associated with ENSO forcing. *Tellus A.* 61, 343–356. doi: 10.1111/j.1600-0870.2008.00387.x

Tropical Rainfall Measuring Mission (TRMM) (2011). TRMM (TMPA) Rainfall Estimate L3 3 hour 0.25 degree x 0.25 degree V7, Greenbelt, MD, Goddard Earth Sciences Data and Information Services Center (GES DISC), (accessed February 20, 2022).

Uribe, E. M. (2002). *El inicio de la temporada de lluvias en la costa sudoeste de México: relaciones para su diagnóstico y pronóstico*. Master dissertation. Mexico City, Mexico: Universidad Nacional Autónoma de México.

Waliser, D. E., and Gautier, C. (1993). A Satellite-Derived Climatology of the ITCZ. *J. Clim.* 6, 2162–2174. doi: 10.1175/1520-0442(1993)006<2162:ASDCOT>2.0.CO;2

Wang, C. (2007). Variability of the Caribbean Low-Level Jet and its relations to climate. *Clim. Dyn.* 29, 411–422. doi: 10.1007/s00382-007-0243-z

Yamada, T. (2015). "Global hydrological cycle and its predictability associated with human activities, Uncertainty of Rainfall-Runoff Process," in *The 18th SNU-HU Joint Symposium*.